Anna Dowierciał, Adam Jarmuła, Piotr Wilk, Wojciech Rypniewski, Borys Kierdaszuk and Wojciech Rode*

Crystal structures of complexes of mouse thymidylate synthase crystallized with N^4-OH-dCMP alone or in the presence of $N^{5,10}$-methylenetetrahydrofolate

Abstract: To solve the inhibition mechanism of thymidylate synthase (TS) by N^4-hydroxy-dCMP (N^4-OH-dCMP), crystallographic studies were undertaken. Structures of three mouse TS (mTS) complexes with the inhibitor were solved, based on crystals formed by the enzyme protein in the presence of either only N^4-OH-dCMP [crystal A, belonging to the space group C 1 2 1, with two monomers in asymmetric unit (ASU), measured to 1.75 Å resolution] or both N^4-OH-dCMP and $N^{5,10}$-methylenetetrahydrofolate (mTHF) (crystals B and C, both belonging to the space group C 2 2 21, each with a single monomer in ASU, measured to resolution of 1.35 Å and 1.17 Å, respectively). Whereas crystal A-based structure revealed the mTS-N^4-OH-dCMP binary complex, as expected, crystals B- and C-based structures showed the enzyme to be involved in a ternary complex with N^4-OH-dCMP and noncovalently bound dihydrofolate (DHF), instead of expected mTHF, suggesting the inhibition to be a consequence of an abortive enzyme-catalyzed reaction, involving a transfer of the one-carbon group to a hitherto unknown site and oxidation of THF to DHF. Moreover, both C(5) and C(6) inhibitor atoms showed *sp3* hybridization, suggesting C(5) reduction, with no apparent indication of C(5) proton release. In accordance with our previous results, in all subunits of these structures the inhibitor molecule was identified as the *anti* rotamer of imino tautomer, forming, similar to deoxyuridine monophosphate, two hydrogen bonds with a conservative asparagine (mouse Asn220) side chain.

Keywords: 3D structure; inhibition; thymidylate synthase.

Enzymes: thymidylate synthase (EC 2.1.1.45).

PDB reference: thymidylate synthase; 4EIN (the crystal A-based structure); 4EZ8 (the crystal C-based structure).

*Corresponding author: Wojciech Rode, Nencki Institute of Experimental Biology, Polish Academy of Sciences, 3 Pasteur Street, 02-093 Warsaw, Poland, Fax: +48-22-822-5342, E-mail: rode@nencki.gov.pl

Anna Dowierciał, Adam Jarmuła and Piotr Wilk: Nencki Institute of Experimental Biology, Polish Academy of Sciences, Warsaw, Poland
Wojciech Rypniewski: Institute of Bioorganic Chemistry, Polish Academy of Sciences, Poznan, Poland
Borys Kierdaszuk: Warsaw University, Institute of Experimental Physics, Warsaw, Poland

Introduction

Thymidylate synthase (TS; EC 2.1.1.45), a target in chemotherapy, catalyzes the conversion of deoxyuridine monophosphate (dUMP) and $N^{5,10}$-methylenetetrahydrofolate (mTHF) to deoxythymidine monophosphate (dTMP) and dihydrofolate (DHF) via reductive methylation, in which mTHF serves as both methyl donor and reducing agent [1].

N^4-hydroxy-dCMP (N^4-OH-dCMP) is a substrate analog, reported to inhibit the enzyme from bacterial, avian and mammalian sources, as well as from certain helminths; inhibition is found to be competitive with respect to dUMP, time- and mTHF-dependent, and accompanied by formation of a ternary complex, N^4-hydroxy-dCMP-mTHF-enzyme, with apparently differing interactions between the low-molecular weight components and each of the two enzyme subunits [2–6]. Similar to FdUMP, incubated with the cofactor and the enzyme N^4-OH-dCMP formed a ternary complex. However, when N^4-OH-[5-³H]dCMP replaced dUMP in the reaction mixture, ³H abstraction from the uracil ring C(5) was not apparent, suggesting the reaction to be inhibited at an earlier stage than with FdUMP. In solution the equilibrium between rotamers (Figure 1) around the C^4-N^4 bond is significantly shifted towards *syn* rotamer [relative to pyrimidine N(3)] [7, 8], but surprisingly only the *anti* isomer appeared to be the active inhibitor form [4].
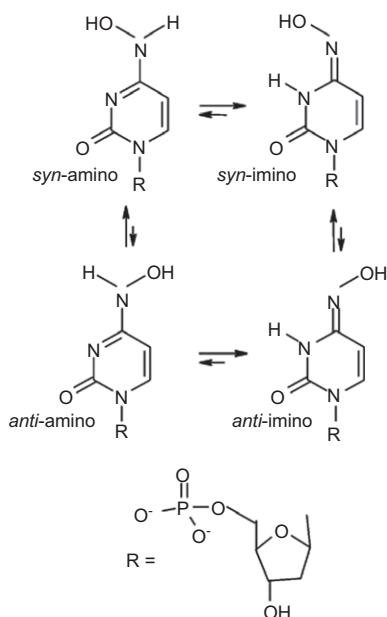
Figure 1 Amino-imino and *syn-anti* equilibria for N⁴-hydroxy derivatives of dCMP.

To learn more about the inhibition mechanism, structural studies of TS complexes with N⁴-OH-dCMP were undertaken.

Materials and methods

Crystallization and data collection

Mouse TS (mTS) recombinant protein, overexpressed and purified as previously described [9], was dialyzed against 5 mM Tris HCl buffer, pH 7.5, containing 5 mM DTT and then concentrated using Amicon Centricon centrifugal filter. Crystals were grown by the vapor diffusion method in hanging drops at approximately 4°C (crystal A)/7°C (crystals B and C) at the following conditions. For two-molecules complex of mTS with N⁴-hydroxy-dCMP, a drop of protein solution of 30 mg/mL concentration containing inhibitor of 6 mM was mixed 1:1 with well solution (0.1 M Mes pH 6.5; 0.2 M MgAcetate; 13.5% PEG 8000) and allowed to equilibrate with 0.5 mL of well solution. In the case of crystals B and C, equal volumes of protein solution of 16.3 mg/mL concentration and well solution were mixed and allowed to equilibrate with 0.5 mL of well solution, containing 0.1 M Mes, pH 6.5/crystal B or pH 6.7/crystal C; 0.06 M MgAcetate and 16% (w/v) PEG 8000.

X-ray diffraction data were collected from single flash-frozen crystals (A, B and C) at the Bessy Synchrotron using X-rays of 0.918 Å wavelength.

Data processing: structure determination and refinement

Data were processed with Denzo and Scalepack [10]. The crystal A-based structure was determined by refining the model of mTS

complexed with SO4²⁻ (PDB ID: 3IHI) relative to the new data. In the case of crystal B, the structure was determined by molecular replacement carried out with the Phaser from CCP4 package [11], using the model of mTS-N⁴-hydroxy-dCMP as the search model. The crystal C-based structure was determined by refining the model of crystal B-based structure with respect to the new data.

The correctness of these structures was evaluated using Sfcheck and Procheck from the CCP4 suite. Some X-ray data and model refinement parameters are summarized in Table 1.

Results and discussion

Structures of three mTS complexes with the inhibitor were solved, based on crystals formed by the enzyme protein in the presence of either only N⁴-OH-dCMP [crystal A, belonging to the space group C 1 2 1, with two monomers in asymmetric unit (ASU), measured to 1.75 Å resolution] or both N⁴-OH-dCMP and mTHF (crystals B and C, both belonging to the space group C 2 2 21, each with a single monomer in ASU, measured to resolution of 1.35 Å and 1.17 Å, respectively). For both subunits of the dimer structure of the mTS-N⁴-OH-dCMP binary complex (structure A), the electron density map is well defined and continuous for the entire molecules of ligand and throughout the protein chains, except for poorly defined loops Glu 42-Thr 47. The mTS-N⁴-OH-dCMP structure is very similar to that of an analogous mTS complex with the substrate, dUMP [9] (Figure 2), as indicated by C_α root mean square deviation (RMSD) between subunits A of both structures amounting to 0.33 Å. Both structures show the protein in the active conformation, with the catalytic Cys 189 located in the active site and extended towards the ligands (Figure 3). The distances between the C6 atoms in the pyrimidine rings of N⁴-OH-dCMP and the sulfur atoms of Cys 189 are 2.87 and 2.94 Å in subunits A and B, respectively, showing the lack of bonding between the enzyme and ligand, as in the mTS-dUMP structure. The molecules of dUMP and N⁴-OH-dCMP preserve virtually the same positions (Figures 2 and 3), both being anchored in the active site by their phosphate moieties, each forming several H-bonds with the quartet of arginines of both TS subunits (Arg 44 and Arg 209 from one subunit and Arg 169′ and Arg 170′ from the other subunit) and a single serine (Ser 210) (not shown). Comparison of the active sites of both structures (Figure 3) reveals different positions of two conservative water molecules. The lower cyan molecule in Figure 3 is located at a H-bond distance from the uracil O4 atom of dUMP. In the mTS-N⁴-OH-dCMP structure this water molecule (lower green) appears to be displaced by approximately 2.3 Å, thus being able to participate in a modified H-bonding network between the N⁴-OH group of N⁴-OH-dCMP and the

Table 1 Data collection and refinement statistics for mTS-N⁴-OH-dCMP (crystal A) and mTS-N⁴-OH-dCMP-DHF (crystals B and C) structures.

	mTS-N⁴-OH-dCMP (crystal A)	mTS-N⁴-OH-dCMP-DHF (crystal B)	mTS-N⁴-OH-dCMP-DHF (crystal C)
Lattice type	Monoclinic	Orthorhombic	Orthorhombic
Space group	C 1 2 1	C 2 2 21	C 2 2 21
Unit cell parameters	a=160.02 Å	a=71.297 Å	a=71.121 Å
	b=87.96 Å	b=111.931 Å	b=112.045 Å
	c=68.67 Å	c=88.237 Å	c=88.297 Å
	$\alpha=90.00°$	$\alpha=\alpha=\gamma=90.00°$	$\alpha=\alpha=\gamma=90.00°$
	$\beta=96.44°$		
	$\gamma=90.00°$		
Resolution range, Å	20–1.75	28.46–1.35	21.35–1.17
No. of unique reflections	90, 892	77, 525	117, 370
Redundancy	2.2	7.1	5.4
$< I/\sigma(I) >$	10.1	11.9	9.8
No. of reflections used in refinement	86, 322	73, 587	117, 324
R factor, %	20.6	10.4	10.7
R_{free} factor, %	25.5	13.1	13.0
RMS bond, Å	0.024	0.023	0.023
RMS angle, °	1.973	2.066	2.013

conservative Glu 81 side chain. The second conservative water molecule has also been displaced from the higher cyan position in mTS-dUMP to higher green position in mTS-N⁴-OH-dCMP, presumably to stabilize an alternative conformation of the Ser 223 side chain in the latter structure. Our model of the mTS-N⁴-OH-dCMP complex shows that the inhibitor molecule preserves the hydrogen bonds [from N(3)-H and N(4) of the cytosine base] to the highly conservative Asn 220, complying with the mechanism of substrate orientation and recognition by TS [12–14].

Structures B and C showed the enzyme to be involved in a ternary complex with N⁴-OH-dCMP and dihydrofolate
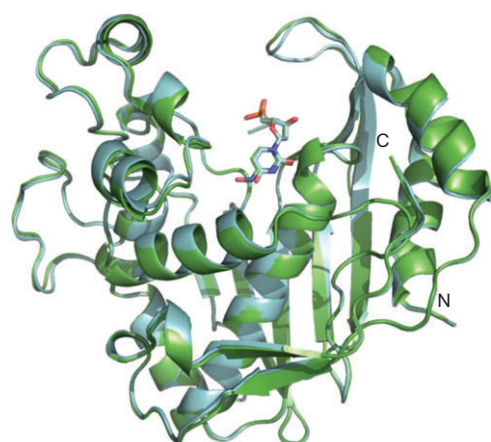

Figure 2 Superimposition of subunits A in mTS-N⁴-OH-dCMP (green) and mTS-dUMP (cyan) complexes. Ligands, N⁴-OH-dCMP and dUMP, are shown as sticks. C- and N-termini of the protein chain are marked.

(DHF). These two structures are virtually identical; therefore, only structure C, solved with better resolution (1.17 Å), will be discussed. The electron density map in mTS-N⁴-OH-dCMP-DHF is very well defined and continuous throughout the protein chains and ligand molecules, except for the glutamate portion of DHF with the electron density less clear and temperature B factors relatively high, the latter suggesting that the glutamate may (partially) occupy at least two conformations that have been consequently modeled in this work. The model shows the protein in the active conformation. Unlike with the mTS-N⁴-OH-dCMP structure, although, the active site in the mTS-N⁴-OH-dCMP-DHF structure is closed, the catalytic Cys 189 being covalently bound to the C(6) atom of N⁴-OH-dCMP, reflected by the continuous electron density and distance of 1.87 Å between the C(6) and Cys 189 sulfur. Similar to the ligand molecules in the mTS-dUMP [9] and mTS-N⁴-OH-dCMP binary complexes, as well as dUMP molecule in the mTS-dUMP-ZD1694 ternary complex (PDB ID: 4EB4) (A. Dowiercial et al., unpublished), the molecule of N⁴-OH-dCMP is anchored in the active site by several H-bonds to its phosphate moiety from a group of four arginines and single serine (not shown). In accordance with our previous results [4] and molecular dynamics simulations results (A. Jarmuła et al., unpublished), the inhibitor molecule adopts the *anti* rotameric form in both the mTS-N⁴-OH-dCMP-DHF and mTS-N⁴-OH-dCMP structures.

The cofactor molecule is bound in the active site with the help of a single water-bridged H-bond between its
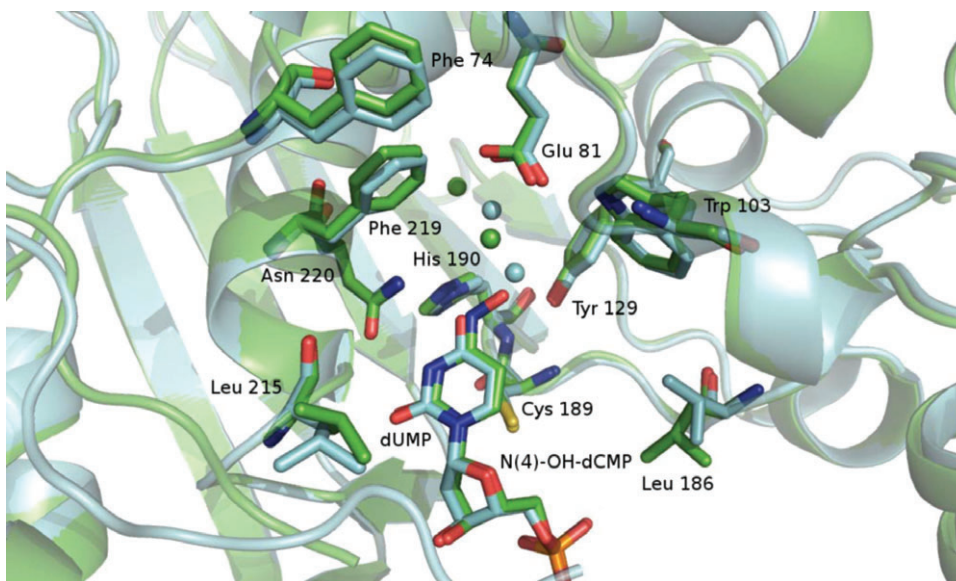
Figure 3 Differences in the active site arrangements in mTS-N⁴-OH-dCMP (green) against mTS-dUMP (cyan). Shown are N⁴-OH-dCMP, dUMP, several amino acids and a few ordered water molecules.

glutamate α-carboxylic group and the side chain of Lys 71 (not shown). This H-bond confirms the postulated role of Lys 71 in the binding of the cofactor molecule [15]. Surprisingly, the electron density in the mTS-N⁴-OH-dCMP-DHF structure indicates the presence of noncovalently bound DHF, instead of expected mTHF (present in the crystallization buffer), suggesting the inhibition to be a consequence of an abortive enzyme-catalyzed reaction, involving a transfer of the one-carbon group to a hitherto unknown site and oxidation of tetrahydrofolate (THF) to DHF. Moreover, both C(5) and C(6) inhibitor atoms showed *sp3* hybridization (cf. [3]), suggesting C(5) reduction and no

indication of proton release from C(5) was apparent. Analysis of the electron density map showed no indication of a possible location of the one-carbon group released from the mTHF cofactor molecule.

The superimposition of the structures of mTS-N⁴-OH-dCMP and mTS-N⁴-OH-dCMP-DHF is shown in Figure 4. The C_α RMSD between both structures is 0.603 Å for subunits A and 0.449 Å for subunits B of the dimeric mTS protein. The most pronounced differences concern the C-terminus (residues Met 305, Ala 306 and Val 307) that is largely shifted in the ternary compared to binary complex, thus contributing to the active site closing. The other differences concern regions adjacent to the active site cleft. In the ternary compared to binary complex, some neighboring residues extend to the inside of the cleft, causing its narrowing (e.g., residues Leu 186, Phe 111, Leu 115) and/or stabilizing the hydrophobic *para*-aminobenzoic acid ring of the DHF molecule (residues Leu 215, Phe 219, Ile 102). Further stabilization of the position of the DHF molecule is provided with water-mediated hydrogen bonding connecting the N1, N2 and N3 atoms of the cofactor pterine ring with protein residues of Asp 212, Ala 306 and Arg 44 (Figure 5).
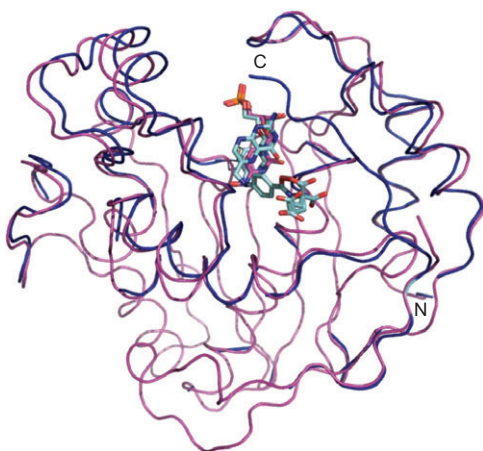
Figure 6 shows an important H-bonding network involving four water molecules (from which only one, W 405, does not have an equivalent in the binary complex), conservative residues of Cys 189, Tyr 129, Glu 81 and Asn 220, and the ligands, N⁴-OH-dCMP and DHF. Interestingly, the postulated molecule of water 405 exhibits only half-occupation, despite its apparently central role
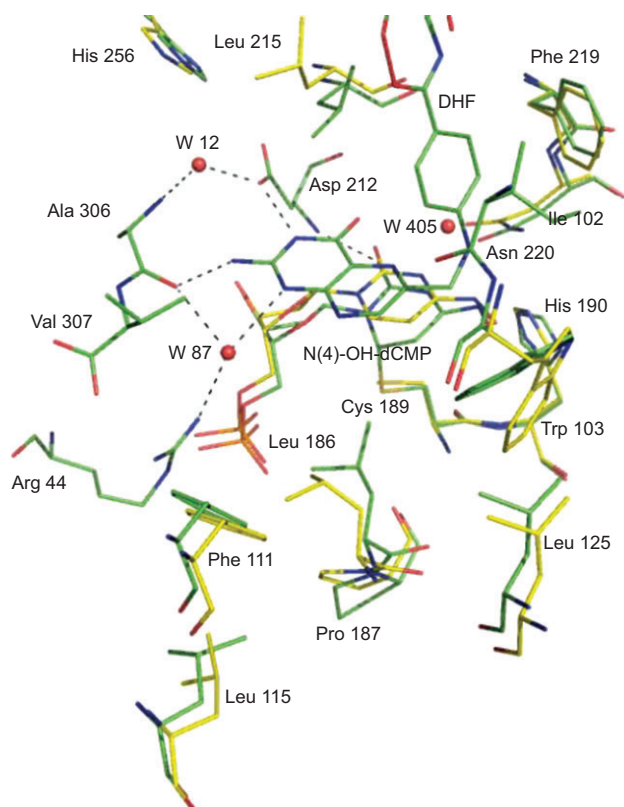

Figure 4 Superimposition of subunits A (the corresponding subunits in both structures) in the mTS-N⁴-OH-dCMP (pink) and mTS-N⁴-OH-dCMP-DHF (blue) complexes. Ligands, N⁴-OH-dCMP and DHF, are shown as sticks. C- and N-termini of the protein chain are marked.

Figure 5 The active site of the mTS-N⁴-OH-dCMP-DHF complex (residues colored in green). Selected residues from the superimposed mTS-N⁴-OH-dCMP complex and the N⁴-OH-dCMP molecule are colored yellow. Selected water molecules are shown as red balls.

in mediating the aforementioned H-bonding network, wherein W 405 serves as a H-bond donor to DHF N5 and N⁴-OH-dCMP N4, as well as H-bond acceptor from DHF N10 and the amine group of Asn 220. The N⁴-OH-dCMP N4-W 405-Asn 220 H-bond shows a better geometrical fit and seems to be preferred over a direct (non-water-mediated) H-bond between N⁴-OH-dCMP N4 and Asn 220, present in the mTS-N⁴-OH-dCMP structure. It is worth noting that molecule W 405, located nearby the N5 and N10 atoms of the cofactor, appears unique among the hitherto investigated binary and ternary complexes of thymidylate synthases from different sources. Similarly located water molecules have been found only in three structures from the Protein Data Bank {EcTS-dUMP-THF, PDB ID: 1KZI [16], EcTS-5-nitro-dUMP-THF, PDB ID: 3BHL (unpublished), and LcTS-dTMP-DHF, PDB ID: 1LCB [17]}, none of which was found directly hydrogen bonded to the cofactor. The
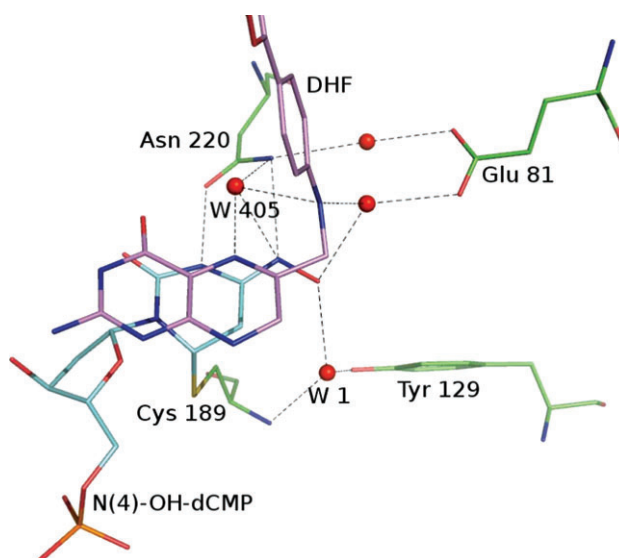

Figure 6 Hydrogen bonding network in mTS-N⁴-OH-dCMP-DHF connecting the ligands (N⁴-OH-dCMP and DHF) with nearby amino acids (Asn 220, Glu 81 and Tyr 129) through ordered water molecules (including W 405 and W 1).

O4 atom in the N⁴-OH group of N⁴-OH-dCMP is stabilized by two hydrogen bonds (forming part of the H-bonding network shown in Figure 6), serving as (i) H-bond donor for one of the water molecules coordinated by the side chain of Gly 81 and N10 of DHF and (ii) H-bond acceptor for water W1, coordinated also by the catalytic Cys 189 and hydroxylic group of Tyr 129. Similar to the binary complex with inhibitor, the N3-H group of N⁴-OH-dCMP in the ternary complex preserves the hydrogen bond to Asn 220. Together, the two structures with the inhibitor, mTS-N⁴-OH-dCMP and mTS-N⁴-OH-dCMP-DHF, preserve, although in slightly different ways, all "conservative" hydrogen bonds formed between the protein and substrate (dUMP) [9]. The latter may explain the distinct preference (exerted in both the binary and ternary complexes) of the mTS protein for binding of the rarely populated anti rotameric form of the N⁴-OH-dCMP molecule.

References

1. Rode W, Leś A. Molecular mechanism of thymidylate synthase-catalyzed reaction and interaction of the enzyme with 2- and/ or 4-substituted analogues of dUMP and 5-fluoro-dUMP. Acta Biochim Pol 1996;43:133–42.

2. Lorenson MY, Maley GF, Maley F. The purification and properties of thymidylate synthetase from chick embryo extracts. J Biol Chem 1967;242:3332–44.

3. Goldstein S, Pogolotti AL, Garvey EP Jr, Santi DV. Interaction of N⁴-hydroxy-2-deoxycytidylic acid with thymidylate synthetase. J Med Chem 1984;27:1259–62.

4. Rode W, Zieliński Z, Dzik JM, Kulikowski T, Bretner M, Kierdaszuk B, et al. Mechanism of inhibition of mammalian tumor and other thymidylate synthases by *N*⁴-hydroxy-dCMP, *N*⁴-hydroxy-5-fluoro-dCMP, and related analogues. Biochemistry 1990;29:10835–42.

5. Rode W, Dąbrowska M, Zieliński Z, Golos B, Wranicz M, Felczak K, et al. Trichinella spiralis and Trichinella pseudospiralis: developmental patterns of enzymes involved in thymidylate biosynthesis and pyrimidine salvage. Parasitology 2000;120:593–600.

6. Felczak K, Miazga A, Poznański J, Bretner M, Kulikowski T, Dzik JM, et al. 5-Substituted N⁴-hydroxy-2′-deoxycytidines and their 5′-monophosphates: synthesis, conformation, interaction with tumor thymidylate synthase, and in vitro antitumor activity. J Med Chem 2000;43:4647–56.

7. Kierdaszuk B, Shugar D. Structure of the planar complex of N4-methoxycytosine with adenine, and its relevance to the mechanism of hydroxylamine mutagenesis. Biophys Chem 1983;17:285–95.

8. Kierdaszuk B, Stolarski R, Shugar D. Hydroxylamine, mutagenesis: observation of inverted Watson-Crick base pairing between N4-methoxyadenosine and adenine with the aid of natural-abundance high-resolution ¹⁵N NMR spectroscopy. Eur J Biochem 1983;30:559–64.

9. Dowiercioł A, Jarmuła A, Rypniewski W, Sokolowska M, Fraczyk T, Ciesla J, et al. Crystal structures of substrate- and sulfate-bound mouse thymidylate synthase. Pteridines 2009;20(Special Issue):163–7.

10. Otwinowski Z, Minor W. Processing of X-ray diffraction data collected in oscillation mode. Methods Enzymol Macromol Crystallogr 1997;276:307–26.

11. Collaborative Computational Project, Number 4. The CCP4 suite: programs for protein crystallography. Acta Cryst 1994;D50:760–3.

12. Finer-Moore JS, Santi DV, Stroud RM. Lessons and conclusions from dissecting the mechanism of a bi-substrate enzyme: thymidylate synthase mutagenesis, function and structure. Biochemistry 2003;42:248–56.

13. Liu L, Santi DV. Exclusion of 2′-deoxycytidine-5′-monophosphate by asparagine 229 of thymidylate synthase. Biochemistry 1993;32:9263–7.

14. Finer-Moore JS, Liu L, Schafmeister CE, Birdsall DL, Mau T, Santi DV, et al. Partitioning roles of side chains in affinity, orientation, and catalysis with structures for mutant complexes: asparagine-229 in thymidylate synthase. Biochemistry 1996;35:5125–36.

15. Arvizu-Flores AA, Sugich-Miranda R, Arreola R, Garcia-Orozco KD, Velazquez-Contreras EF, Montfort WR, et al. Role of an invariant lysine residue in folate binding on Escherichia coli thymidylate synthase: calorimetric and crystallographic analysis of the K48Q mutant. Int J Biochem Cell Biol 2008;40:2206–17.

16. Fritz TA, Liu L, Finer-Moore JS, Stroud RM. Tryptophan 80 and leucine 143 are critical for the hydride transfer step of thymidylate synthase by controlling active site access. Biochemistry 2002;41:7021–9.

17. Finer-Moore JS, Fauman EB, Foster PG, Perry KM, Santi DV, Stroud RM. Refined structures of substrate-bound and phosphate-bound thymidylate synthase from Lactobacillus casei. J Mol Biol 1993;232:1101–16.